Improved Broadband Matching Bound

Ding Nie, *Member, IEEE,* and Bertrand M. Hochwald, *Fellow, IEEE*

***Abstract*—In radio-frequency systems where a load is driven by a source through a passive impedance matching circuit, the bandwidth over which match can be attained is limited. The Bode-Fano upper bound is often invoked to find this limit. We show that the bound is loose for some loads, and hence cannot be attained by any network. We present a simple method to improve the bound, and give conditions under which the improved bound is tight. The improved bound requires no additional assumptions or conditions beyond what is used for the Bode-Fano bound. Applications to analytical and numerical load models are demonstrated.**

***Index Terms*—Bandwidth, Bode-Fano bounds, lossless matching networks, Rouché's Theorem**

I. Introduction

When a radio-frequency (RF) source is used to drive a load whose impedance varies with frequency, an impedance matching network is generally used to facilitate power transfer between the two. However, a close match can generally be attained only over a limited bandwidth. One measure of the maximum achievable bandwidth is given by the Bode-Fano upper bound [1], [2]. This bound is calculated using the frequency characteristics of the load, and gives us the highest bandwidth achievable by any passive matching network.

Since the introduction of the Bode-Fano bound, it has been extended in many ways, including for sources with frequency-dependent impedances [3]–[5], and for multiport systems where multiple loads are driven by multiple sources [6]–[9]. Recently, [10] showed that tighter bound than the original Bode-Fano bound can be obtained for some loads.

Various methods are available to design two-port matching networks that have wide bandwidth, such as by using Chebyshev networks [2], [11]–[14] and numerical methods [15]–[22]. However, no method is guaranteed to achieve the bound. In fact, for some loads the bound is loose and cannot be achieved by any passive network.

We extend the work in [10] and present a method to determine when the bound is loose. We then show how it may be improved (tightened), and give conditions under which this bound is tight. We employ a tool from complex analysis—Rouché's Theorem [23]. The reader may see the improved bound statement and steps for how to compute it in Sections III-C and III-D. The improved bound requires no additional assumptions or conditions beyond what is used for the Bode-Fano bound.

D. Nie is with Apple Inc., Cupertino, CA 95014, USA (e-mail: kirknie@gmail.com).

B. M. Hochwald is with the Department of Electrical Engineering, University of Notre Dame, Notre Dame, IN 46556, USA (e-mail: bhochwald@nd.edu).

This work was supported, in part, by NSF grants CCF-1403458 and ECCS-1509188.

We illustrate the improved bound in two ways. First, we apply it to an analytical load model of a two-stage resistor-capacitor (RC) load. This load is a simple extension of the classical RC load that is commonly used to illustrate the Bode-Fano bound. We show that the Bode-Fano bound is loose in this example, and that the improved bound is actually one-third of the original bound. An example matching scheme is also presented to show that the improved bound is tight.

Second, we apply the improved bound to a realistic load that is described numerically by its impedance as a function of frequency. The process of applying the bound to such a load requires fitting an equivalent circuit or rational model. The amount of improvement then depends on details of the resulting rational model.

Section II summarizes the Bode-Fano bound, presents the conditions for achieving the bounds, and shows how to determine if the bound is loose. In Section III, we present the improved bound; the crux of the method is to apply Rouché's Theorem to show that one of the conditions for achieving the bound cannot be met in some cases. Analytical and numerical examples are presented in Section IV. Section V concludes.

II. Bode-Fano Bound

A. System description

We consider the RF system shown in Figure 1, where a dissipative load is driven by a source with real impedance Z_0, the characteristic impedance of the system. Let $S_L(s)$ be the reflection coefficient of the load as a rational function of the complex frequency $s = \sigma + j\omega$, where σ and ω are real. $S_L(s)$ is obtained by extending the reflection coefficient of the load $S_L(j\omega)$ as a function of the radian frequency ω to the whole complex plane. Mathematically, $S_L(s)$ can be thought of as the transfer function between the incident and reflected waves ae^{st} and be^{st} to and from the load (see Figure 1), which may have an exponentially increasing or decreasing component, where t represents time. Therefore, we have $b(s) = S_L(s)a(s)$. The impedance $Z_L(s)$ of the loads can be obtained by $Z_L(s) = Z_0(1 + S_L(s))/(1 - S_L(s))$.

Many antenna and distributed-element loads do not have rational descriptions of their S-parameters for all frequency. In such cases, the non-rational description of the load must be approximated by a rational $S_L(s)$ over a frequency range of interest. We do not discuss the issue of rational approximation or calculation of the error tolerance herein since they are addressed extensively elsewhere. An early example is [24], and a summary of some practical techniques can be found in [25]. Other fields such as control engineering use rational fitting extensively [26]. We assume herein that a rational $S_L(s)$ has been chosen to adequately describe the load.

A lossless two-port matching network is inserted to match the impedances between the source and the load, as indicated

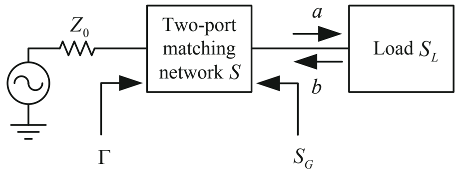

Fig. 1. An RF system where a source with characteristic impedance Z_0 drives a load with reflection coefficient S_L through a lossless two-port matching network with 2×2 S-matrix S (the complex-frequency argument s is omitted). Let a and b be the incident and reflected waves to and from the load. The reflection coefficients seen from the input and output ports of the matching network are denoted as Γ and S_G, respectively.

in Figure 1. We use $S(s)$ to denote the 2×2 S-matrix of the matching network as a function of s, whose entries are $S_{ij}(s)$ where $i,j=1,2$. Let $\Gamma(s)$ be the reflection coefficient of the cascade of $S(s)$ and $S_L(s)$, and $S_G(s)$ be the reflection coefficient seen from the output port of the matching network. It follows that $S_G(s)=S_{22}(s)$, and

$$\Gamma(s) = S_{11}(s) + \frac{S_{12}(s)S_L(s)S_{21}(s)}{I - S_G(s)S_L(s)}. \tag{1}$$

Since the matching network is lossless, the incident power to the network is either transferred to the load or reflected back to the source. The matching between source and load at $s=j\omega$ can therefore be measured by the return loss $|\Gamma(j\omega)|$. By definition, $0 \le |\Gamma(j\omega)| \le 1$ where values close to zero indicate that little power is being reflected and most of the source power is being delivered to the loads. Generally, values close to zero over a wide range of ω are preferred.

We use LHP to denote the left-half complex plane ($\mathrm{Re}\{s\} < 0$) and RHP to denote the right-half ($\mathrm{Re}\{s\} > 0$). The $j\omega$ axis is not included in either the LHP or the RHP. Because the load is dissipative and the matching network is lossless, $S_L(s)$ and $S(s)$ are real-rational, Hurwitzian, bounded, and $S(s)$ is para-unitary; the definitions of these terms may be found readily in [27]–[29].

As a result of these properties, $S_L(s)$ and $S_G(s)$ are rational functions of s, their poles are in the LHP, their poles and zeros are in complex conjugate pairs, and $|S_L(s)| < 1$, $|S_G(s)| < 1$ for $\mathrm{Re}\{s\} > 0$. This latter property is especially important in our discussion. The poles and zeros of $S_L(s)$ are denoted $p_{L,i}$ and $z_{L,i}$, $i=1,2,\ldots$.

B. Bode-Fano bound statement

For a load $S_L(s)$, we assume that there exists an s_0 with $\mathrm{Re}\{s_0\} \ge 0$ or $s_0 = \infty$ such that

$$S_L(-s_0)S_L(s_0) = 1. \tag{2}$$

Then [2] proves that the following inequality holds for any lossless matching network:

$$\int_0^\infty f(\omega)\log\frac{1}{|\Gamma(j\omega)|}d\omega \le B, \tag{3}$$

where the functional forms of $f(\omega) > 0$ and $B > 0$ depend on s_0; see Table I. Equality in (3) holds if and only if the following Conditions are satisfied simultaneously:

TABLE I
FORMS OF $f(\omega)$, B AND $g(z)$ FOR DIFFERENT LOCATIONS OF s_0.

$s_0 = j\omega_0$	$f(\omega) = \frac{1}{2}[(\omega_0-\omega)^{-2} + (\omega_0+\omega)^{-2}]$
	$B = -\frac{\pi}{2}\left[\sum_i (p_{L,i} - j\omega_0)^{-1} + \sum_i (z_{L,i} + j\omega_0)^{-1}\right]$
	$g(z) = -\frac{\pi}{2}\left[(z-j\omega_0)^{-1} + (z+j\omega_0)^{-1}\right]$
$\mathrm{Re}\{s_0\} > 0$	$f(\omega) = \frac{1}{2}\mathrm{Re}[(s_0-j\omega)^{-1} + (s_0+j\omega)^{-1}]$
	$B = -\frac{\pi}{2}\log\left\lvert \det S_L(s_0)\cdot\frac{\prod_i (s_0+z_{L,i})}{\prod_i (s_0-z_{L,i})}\right\rvert$
	$g(z) = -\frac{\pi}{4}\log\left\lvert\frac{(s_0+z)(s_0+z^*)}{(s_0-z)(s_0-z^*)}\right\rvert$
$s_0 = \infty$	$f(\omega) = 1$
	$B = -\frac{\pi}{2}\left(\sum_i p_{L,i} + \sum_i z_{L,i}\right)$
	$g(z) = -\pi z$

1) $S_L(s_0)S_G(s_0) \ne 1$
2) $S_L(s) - S_G(-s)$ has no zeros in the LHP

These Conditions are discussed in detail in Section III.

The physical meaning of the assumption (2) is most easily understood when $s_0 = j\omega_0$ ($\mathrm{Re}\{s_0\} = 0$). Because $S_L(-j\omega_0) = S_L^*(j\omega_0)$, where * represents complex conjugation, it follows from (2) that $|S_L(s_0)| = 1$. Thus, s_0 is a frequency where the load reflects all incident energy. There may be multiple such s_0. We simply assume there is at least one.

C. Discussion of bound

As shown in [2], the Bode-Fano bound is the result of the inequality

$$\int_0^\infty f(\omega)\log\frac{1}{|\Gamma(j\omega)|}d\omega \le B - \sum_i g(z_i), \tag{4}$$

where z_i, $i=1,2,\ldots$ are the LHP zeros of $S_L(s) - S_G(-s)$, and $g(z) > 0$ is given in Table I. Equality in (4) holds if and only if $S_L(s_0)S_G(s_0) \ne 1$.

Since $g(z_i)$ depends on z_i, which depends on the matching network, the right hand side of (4) depends on the choice of network. Setting $\sum_i g(z_i) = 0$ yields (3), which is independent of the matching network and therefore holds for any network.

The bound requires a rational $S_L(s)$. To apply the bound to loads whose frequency response is obtained from either measurements or simulations, a rational function approximation is needed. This approximation can be obtained as follows:

a) Measure or simulate the S-parameter of the load in some frequency range $\omega \in [\omega_1, \omega_2]$. Denote the response as $S_L'(j\omega)$.
b) Find a passive rational $S_L(s)$ such that $|S_L'(j\omega) - S_L(s)|$ is within an error tolerance for $s = j\omega$ and $\omega \in [\omega_1, \omega_2]$.

Step a) can be done with standard modeling software such as Ansys HFSS in the case of simulations, or a network analyzer in the case of measurements. Step b) can be accomplished by finding rational approximations to $S_L'(j\omega)$ using, for instance, the Matrix Fitting Toolbox [30]–[34] in MATLAB. A study of the accuracy of approximation and its effect on the bound calculation can be found in [9], and is omitted here.

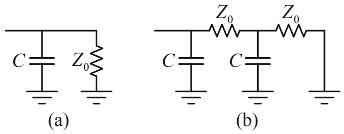

Fig. 2. (a) Classical circuit-model of a load consisting of a capacitor C in parallel with the characteristic impedance Z_0. (b) Simple extension of the load in (a) to two cascaded RC stages.

D. Canonical application

We briefly describe a canonical application of the bound that we carry forward to the next section and the improved bound. For a load that is a perfect reflector at $s_0 = \infty$, taking $f(\omega) = 1$ from Table I (third row) and calculating (3) obtains

$$\int_0^\infty \log \frac{1}{|\Gamma(j\omega)|} d\omega \leq B = -\frac{\pi}{2}\left(\sum_i p_{L,i} + \sum_i z_{L,i}\right). \quad (5)$$

It is typically desired to create a matching network operating over some band $\omega \in [\omega_1, \omega_2]$. Since $0 \leq |\Gamma(j\omega)| \leq 1$, and therefore $f(\omega)\log(1/|\Gamma(j\omega)|) \geq 0$, then constraining the range of integration in (5) gives

$$\int_{\omega_1}^{\omega_2} \log \frac{1}{|\Gamma(j\omega)|} d\omega \leq B \quad (6)$$

For a matching circuit where $|\Gamma(j\omega)| \leq \tau$ for $\omega \in [\omega_1, \omega_2]$, where τ is typically a small value that represents the maximum desired reflection in the band of interest, (6) yields

$$\omega_2 - \omega_1 \leq \frac{-\frac{\pi}{2}\left(\sum_i p_{L,i} + \sum_i z_{L,i}\right)}{\log(1/\tau)}.$$

For $s_0 \neq \infty$, other bandwidth bounds can be obtained using (3). We refer the reader to [2].

A circuit-model load often used to exemplify the bound is shown in Figure 2(a) consisting of a capacitor C in parallel with the characteristic impedance Z_0. From this model, the impedance of the load is $Z_L(s) = Z_0/(Z_0Cs + 1)$. Therefore

$$S_L(s) = \frac{Z_L(s) - Z_0}{Z_L(s) + Z_0} = \frac{-Z_0Cs}{Z_0Cs + 2}. \quad (7)$$

Following the steps for calculating the bound, we obtain $s_0 = \infty$, $p_{L,1} = -2/(Z_0C)$ and $z_{L,1} = 0$. Hence, the bound for the single-stage RC load is

$$B_1 = \frac{\pi}{Z_0C}. \quad (8)$$

(We use the subscript "1" to refer to the single-stage.)

We contrast this result with the load shown in Figure 2(b) comprising two cascaded identical RC structures. The reflection coefficient of the load is

$$S_L(s) = \frac{-Z_0^2C^2s^2 - 2Z_0Cs + 1}{Z_0^2C^2s^2 + 4Z_0Cs + 3}. \quad (9)$$

Similarly to the load in Figure 2(a), this load satisfies (2) at $s_0 = \infty$. Solving for the poles and zeros of $S_L(s)$ yields

$$p_{L,1} = -\frac{3}{Z_0C}, p_{L,2} = -\frac{1}{Z_0C}, z_{L,1}, z_{L,2} = \frac{-1 \pm \sqrt{2}}{Z_0C}$$

The bound for this load is then

$$B_2 = \frac{3\pi}{Z_0C}. \quad (10)$$

Because (10) is three times larger than (8), it would appear that the bandwidth achievable with the load model in Figure 2(b) is three times larger than Figure 2(a). As we show, however, their achievable bandwidths are actually equal, and the improved bound reveals this.

III. Improved Bound

The derivation of the Bode-Fano bound in (3) relies on replacing the non-negative term $\sum_i g(z_i)$ in (4) that depends on the matching network with zero. An improved bound that applies to all matching networks can therefore, in principle, be obtained by replacing $\sum_i g(z_i)$ instead with a positive value, provided that this value is also independent of the matching network. We find such a value by a careful examination of the conditions for achieving equality in (3).

A. Condition 1 for equality can always be met

Condition 1 is a "non-degenerate" condition described in detail in [2]. It turns out that Condition 1 is superfluous when $\text{Re}\{s_0\} > 0$ because $S_L(s)$ and $S_G(s)$ are bounded functions; hence $S_L(s)S_G(s)$ is also bounded and $|S_L(s_0)S_G(s_0)| < 1$ for $\text{Re}\{s_0\} > 0$. However, for other values of s_0, this condition needs to be checked.

In the RC example in Figure 2(a), $S_L(s)$ is reflective at $s_0 = \infty$ because the load is capacitive relative to ground and presents a short circuit as the frequency tends to infinity ($S_L(\infty) = -1$). In order for Condition 1 to hold, we need to make sure that $S_G(\infty) \neq -1$. Because $S_G(s)$ represents the reflection coefficient seen from the output of the matching network (see Figure 1), Condition 1 is satisfied if the output port of the matching network is not also a short at $s = \infty$. Since this is a constraint on the matching network at a single frequency, it can generally be met with little effort.

For example, setting $S_G(s) = 0$ (direct connection of source and load without intervening matching network), achieves Condition 1. As we show in the next section, $S_G(s) = 0$ also achieves Condition 2 for the circuit in Figure 2(a). However, this is not the case for the circuit in Figure 2(b).

B. Condition 2 for equality cannot always be met

Condition 2 is referred to as a "minimum-phase" condition [35] because if there are no LHP zeros of $S_L(s) - S_G(-s)$, then there are no RHP zeros of $S_L(-s) - S_G(s)$, which implies that there are no RHP zeros in the lossless equivalent circuit of the load; see [9]. Compared with Condition 1, the physical meaning of Condition 2 is less clear and designing matching networks to satisfy this condition is not trivial.

For the load in Figure 2(a), from (7) we see that $S_L(s)$ has a single zero at $z_{L,1} = 0$, and no zeros in the LHP. Hence, Condition 2 is trivially satisfied for $S_G(s) = 0$. Thus, Conditions 1 and 2 are satisfied and equality in (8) can be achieved without a matching network. However, if desired,

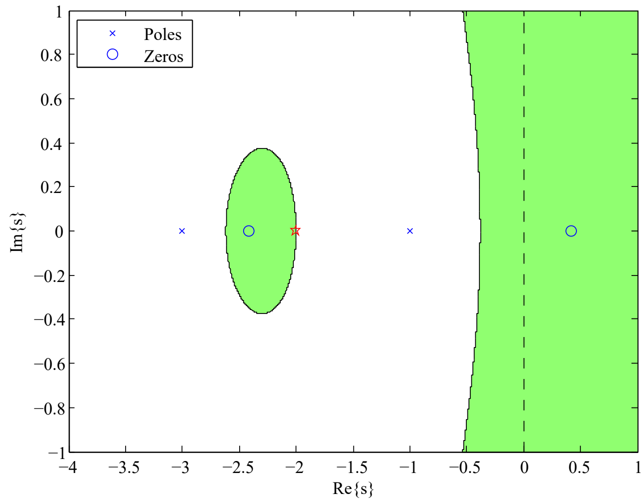

Fig. 3. For the two-stage RC load in Figure 2(b) with $S_L(s)$ in (9), the $|S_L(s)| = 1$ curves are plotted over the s-plane and the $|S_L(s)| < 1$ regions are filled with green. The set of points inside the closed $|S_L(s)| = 1$ contour in the LHP is denoted as Ω_1. The poles and zeros of $S_L(s)$ are marked respectively by crosses and circles; among them, $z_{L,1}$ is located in Ω_1. A pentagram is used to denote $\hat{z}_1$ defined in (14).

matching networks such as Chebyshev networks [2], [11]–[14], can be used to shape the frequency response of the load and still achieve equality.

For the load in Figure 2(b), the situation changes, and Condition 2 cannot be met by any lossless matching network. We use Rouché's Theorem [23] to explain why. This theorem says that if functions $f_1(s)$ and $f_2(s)$ are analytic on some region Ω of the complex plane whose boundary contour is $\partial\Omega$, with $|f_2(s)| < |f_1(s)|$ on $\partial\Omega$, then $f_1(s)$ and $f_1(s) + f_2(s)$ have the same number of zeros in Ω, where each zero is counted as many times as its multiplicity.

Let $f_1(s) = S_L(s)$ and $f_2(s) = -S_G(-s)$. For the circuit-model of Figure 2(b), Figure 3 plots $|S_L(s)| = 1$ contours for (9) over the s-plane. We see that there exists a single closed $|S_L(s)| = 1$ contour contained in the LHP, denoted $\partial\Omega_1$ and whose interior is denoted Ω_1. Moreover, $z_{L,1} = -(1 + \sqrt{2})/(Z_0C)$ is in Ω_1. Since $S_G(s)$ is a bounded function, we have $|f_2(s)| < 1$ for s in the LHP, and since $\partial\Omega_1$ is contained in the LHP, $|f_2(s)| < 1$ for $s \in \{\Omega_1 \cup \partial\Omega_1\}$. Hence, $|f_2(s)| < |f_1(s)| = 1$ for $s \in \partial\Omega_1$, and Rouché's Theorem indicates that $f_1(s) + f_2(s) = S_L(s) - S_G(-s)$ has the same number of zeros for $s \in \Omega_1$ as $f_1(s) = S_L(s)$. Since $S_L(s)$ has one such zero, this means $S_L(s) - S_G(-s)$ also has a zero in Ω_1, no matter what $S_G(s)$ is. Therefore, Condition 2 cannot be met for any lossless matching network.

This example shows not only that $S_L(s) - S_G(-s)$ always has a zero in the LHP, but this zero must lie in Ω_1. We may extend and generalize this analysis for any load to improve the original Bode-Fano bound.

C. Improved bound statement

Let $S_L(s)$ denote the reflection coefficient of the load as a rational function of complex frequency s. Assume that there exists an s_0 with $\mathrm{Re}\{s_0\} \geq 0$ or $s_0 = \infty$ such that

$$S_L(-s_0)S_L(s_0) = 1. \tag{11}$$

Denote $\partial\Omega$ as any closed contour (with interior Ω) that is obtained by solving $|S_L(s)| = 1$ and is contained entirely in the LHP. Let $z_{L,i}$ be a zero of $S_L(s)$ that is contained in some Ω_i, and enumerate all such zeros $z_{L,1}, \ldots, z_{L,\ell}$ and their corresponding $\Omega_1, \ldots, \Omega_\ell$. Then

$$\int_0^\infty f(\omega) \log \frac{1}{|\Gamma(j\omega)|} d\omega \leq B' \tag{12}$$

where

$$B' = B - \sum_{i=1}^{\ell} g(\hat{z}_i) \tag{13}$$

$$\hat{z}_i = \arg\min_{z \in \Omega_i} \mathrm{Re}\{g(z)\}, \tag{14}$$

$\Gamma(j\omega)$ is the reflection coefficient of the cascaded matching network and load defined in (1), and $f(\omega)$, B, and $g(z)$ are calculated using Table I.

Since B and $\hat{z}_i$ depend only on $S_L(s)$, (12) applies to any matching network. Equality in (12) holds if and only if the following two Conditions hold:

1) $S_L(s_0)S_G(s_0) \neq 1$
2′) $S_L(s) - S_G(-s)$ has ℓ LHP zeros $\hat{z}_1, \ldots, \hat{z}_\ell$.

Condition 1 and (11) are similar to requirements needed for the Bode-Fano bound in Section II-B. Condition 2′ differs from Condition 2 for the original bound.

D. Discussion of improved bound

The minima in (14) can be readily computed because $\Omega_1, \ldots, \Omega_\ell$ are surrounded by the closed contours $\partial\Omega_1, \ldots, \partial\Omega_\ell$ in the LHP, and either analytical or numerical methods can be used.

The complete steps for computing the bound are summarized as follows:

1) Find an s_0 where (11) is satisfied for $S_L(s)$.
2) Calculate the poles and zeros $p_{L,i}, z_{L,i}$ of $S_L(s)$, and B from Table I.
3) Find all LHP closed contours where $|S_L(s)| = 1$. Denote any that contain $z_{L,i}$ as $\partial\Omega_i$. If there are no such $\partial\Omega_i$ then $B' = B$.
4) Otherwise calculate $\hat{z}_i$ and $g(\hat{z}_i)$ using (14).
5) Calculate the improved bound B' in (13).

Steps 1 and 2 are used to calculate the original bound in (3), while Steps 3 and 4 improve the bound. Step 3 can be done graphically by drawing the contours $|S_L(s)| = 1$ and examining if any zeros of $S_L(s)$ are enclosed.

E. Derivation of bound

We generalize the analysis of Section III-B by noting that $|S_L(s)| = 1$ is possible only for $\mathrm{Re}\{s\} \leq 0$ because $|S_L(s)| < 1$ for all s in the RHP (this is a consequence of the bounded Hurwitzian properties of these functions). By applying Rouché's Theorem to each $z_{L,i}$ and Ω_i, we conclude that $S_L(s) - S_G(-s)$ has at least ℓ LHP zeros, denoted by $z_1, \ldots, z_\ell$, that satisfy $z_i \in \Omega_i$.

We can now replace the term $\sum_{i=1}^{\ell} g(z_i)$ in (4) with a positive value that is independent of the matching network. Since z_i are in conjugate pairs and $g(z_i)$ in Table I satisfies $g(z_i^*) = (g(z_i))^*$, then $g(z_i) + g(z_i^*) = 2\mathrm{Re}(g(z_i)) \geq \min_{z\in\Omega_i} 2\mathrm{Re}(g(z)) \geq 0$. This yields (12)–(14).

F. Other Bode-Fano inequalities

Our bound analysis requires the assumption (11). If this assumption is strengthened such that $1 - S_L(-s)S_L(s)$ has a zero at $s = s_0$ of multiplicity m greater than one, then [2] shows that inequalities other than (4) can also be derived.

For example, if $m \geq 3$ at $s_0 = \infty$, then the following inequality also holds

$$\int_0^{\infty} \omega^2 \log \frac{1}{|\Gamma(j\omega)|} d\omega \leq \frac{\pi}{6}\left(\sum_i p_{L,i}^3 + \sum_i z_{L,i}^3\right) - \frac{\pi}{3}\sum_i z_i^3, \tag{15}$$

where z_i, $i = 1, 2, \ldots$ are the LHP zeros of $S_L(s) - S_G(-s)$. Equality in (15) holds if and only if $S_L(\infty)S_G(\infty) \neq 1$. Although $\mathrm{Re}\{z_i\} < 0$, we cannot determine the sign of $\mathrm{Re}\{z_i^3\}$ without knowing the imaginary components of z_i. Hence, we cannot derive an upper bound from (15) that is independent of the matching network. We therefore do not pursue (15) any further.

IV. Example Applications

We illustrate applications of the improved bound using analytical and numerical examples.

A. Analytical example

We briefly revisit the one-stage RC example in Figure 2(a). Steps 1 and 2 in Section III-D have already been done using (7). The only zero is $z_{L,1} = 0$, so it is not possible for $z_{L,1}$ to be contained inside any $\partial\Omega_1$ that is in the LHP. Therefore, Step 3 yields no contours and $B_1' = B_1$. But we already know the Bode-Fano bound (8) is tight in this example so this conclusion is unsurprising.

For the two-stage RC example in Figure 2(b), Steps 1 and 2 have already been done using (9). For Step 3, Figure 3 plots the $|S_L(s)| = 1$ curves and the zeros of $S_L(s)$, where $S_L(s)$ is given in (9). From Figure 3, $z_{L,1} = -(1+\sqrt{2})/(Z_0C)$ is in Ω_1. Because $s_0 = \infty$, Table I indicates that $g(z_i) = -\pi z_i$. To find $\hat{z}_1$ in Step 4, $g(\hat{z}_1)$ is minimized by the closest point to the imaginary axis in Ω_1. This point is marked by a pentagram in Figure 3, which is located on the real axis and satisfies $S_L(\hat{z}_1) = -1$. Solving this gives $\hat{z}_1 = -2/(Z_0C)$. Therefore, the improved bound is obtained by subtracting $g(\hat{z}_1)$ from (10) and getting

$$B_2' = \frac{\pi}{Z_0C}. \tag{16}$$

which is one-third of the Bode-Fano bound in (10), and *coincides with* B_1 in (8).

Bound (16) is tight in that it can be approached by choosing a matching network such that $S_G(s) = -1 + \varepsilon$, where $\varepsilon > 0$ is arbitrarily small. For this $S_G(s)$, the LHP zero of $S_L(s) - S_G(-s)$ is at $z_1 = -\frac{2+(\sqrt{1+\varepsilon^2}-1)/\varepsilon}{Z_0C}$, and the achieved integral in (16) is $\frac{\pi-\pi(\sqrt{1+\varepsilon^2}-1)/\varepsilon}{Z_0C} \approx \frac{\pi(1-\varepsilon/2)}{Z_0C}$. Clearly, the smaller ε is, the closer z_1 is to $\hat{z}_1 = -2/(Z_0C)$, and the closer the achieved integral is to bound (16). Hence, Condition 2′ can be asymptotically satisfied as $\varepsilon \to 0$, and bound (16) is tight. However, ε cannot be zero because Condition 1 is violated by $S_G(s) = -1$ since $S_L(s_0)S_G(s_0) = 1$

For example, if we let $\varepsilon = 0.01$, we obtain $S_G(s) = -0.99$ and $z_1 = -2.005/(Z_0C)$. The achieved integral in (16) is therefore $0.995\pi/(Z_0C)$. This $S_G(s)$ can be realized by a matching network consisting of a single ideal transformer whose input to output turn ratio is 14.11 : 1. The impedance seen at the output port of this matching network is a constant resistance $0.005Z_0$.

Since $B_2' = B_1$, it is conceivable that a single matching circuit can be used for either load to achieve comparable bandwidth. We illustrate that this is indeed so with the matching network in Figure 4(a), chosen for $Z_0 = 50\ \Omega$ and $C = 20$ pF in Figure 2. Figure 4(a) represents a fifth-order Chebyshev matching network designed using methods presented in [2], [14].

When applied to the single-stage RC load, the matching network presents an equal-ripple $|\Gamma(j\omega)|$ frequency response between 2.56 GHz and 2.83 GHz (bandwidth of 266 MHz), where $|\Gamma(j\omega)|$ for the RC load is shown by the blue dashed curve in Figure 4(b), and the maximum return loss in the passband is -14 dB. The Chebyshev network achieves the bound $B_1 = \frac{\pi}{Z_0C} = 3.14 \times 10^9$ for the RC load.

For the two-stage RC load in Figure 2(b), the matching network presents a $|\Gamma(j\omega)|$ shown by the red solid curve

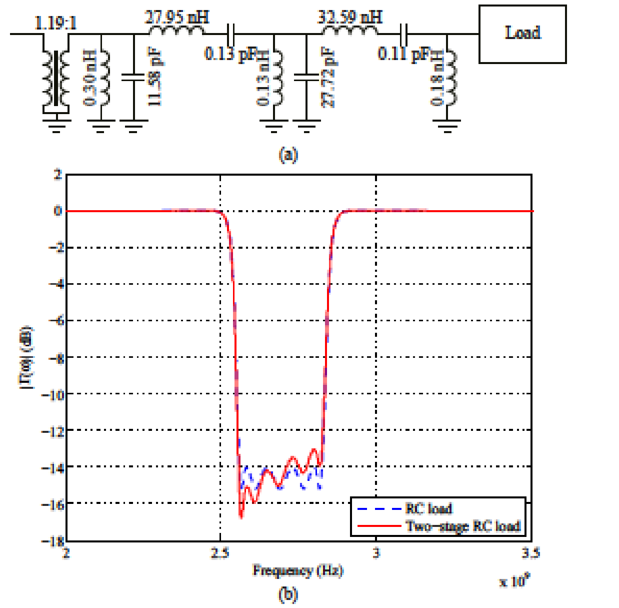

Fig. 4. (a) For the RC load in Figure 2(a), where $Z_0 = 50\ \Omega$ and $C = 20$ pF, a fifth-order Chebyshev network that matches the load between 2.56 GHz and 2.83 GHz is shown. (b) When the network in (a) is used to match both the single-stage and two-stage RC load in Figure 2, the resulting $|\Gamma(j\omega)|$ is plotted versus frequency.

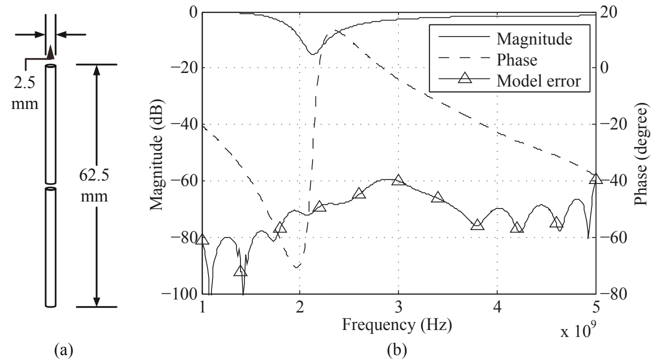

Fig. 5. (a) A dipole that is half-wavelength at 2.4 GHz. (b) For the dipole in (a), the magnitude and phase of the reflection coefficient are plotted in 1–5 GHz. Also shown are the error magnitude of the rational model. The magnitudes refer to the left y-axis and the phase refers to the right.

TABLE II
VALUES OF $p_{L,i}$ AND $z_{L,i}$ FOR THE TWO $S_L(s)$ MODELS IN (17).

i	$p_{L,i}$	$z_{L,i}$
1, 2	$(-3.01 \pm 9.36j) \times 10^9$	$(-3.01 \pm 9.42j) \times 10^9$
3, 4	$(-0.26 \pm 1.25j) \times 10^{10}$	$(-0.05 \pm 1.34j) \times 10^{10}$
5, 6	$(-0.34 \pm 2.57j) \times 10^{10}$	$(-0.35 \pm 2.59j) \times 10^{10}$
7, 8	$(-0.45 \pm 3.30j) \times 10^{10}$	$(-0.54 \pm 3.38j) \times 10^{10}$
9	-4.91×10^{10}	2.14×10^{11}

in Figure 4(b). The passband for the two-stage RC load is approximately the same as that for the single-stage RC load.

It is perhaps surprising that $B_2' = B_1$, but an intuitive explanation proceeds as follows. We know that (8) is tight and can be achieved by connecting the source directly to the load. Clearly, at high frequencies, the capacitor in Figure 2(a) makes the impedance of the parallel circuit small and reactive. The same is true of the circuit in Figure 2(b). For high frequencies, $S_L(s)$ in (7) approximately equals $S_L(s - \frac{2}{Z_0 C})$ in (9). Hence, if the frequency range $[\omega_1, \omega_2]$ is supported by the circuit Figure 2(a), then the same range can be achieved in Figure 2(b), but offset by $2/(Z_0 C)$. A transformer is used in the matching circuit for Figure 2(b) to lower the impedance of the source and, hence, shift the match towards high frequencies. It follows that the transformer used to achieve B_2' also achieves B_1.

We next present a numerical example of the improved bound.

B. Numerical example using realistic load

A dipole antenna is shown in Figure 5(a), which is half-wavelength at 2.4 GHz. To apply the bound, we first simulate the frequency response of the dipole in 1–5 GHz using Ansys HFSS, and then model the reflection coefficient as a rational function. During the modeling process, we can specify the degree of the rational function. Typically, the higher degree we use, the better precision we get from the model. However, there is the risk of "over-fitting", and some guidelines for choosing the degree are found in [9].

We model the reflection coefficient of the dipole using a rational function with degree nine, which has the following form:

$$S_L(s) = k \cdot \frac{\prod_{i=1}^{9}(s - p_{L,i})}{\prod_{i=1}^{9}(s - z_{L,i})}, \tag{17}$$

where $k = -0.19$, and $p_{L,i}, z_{L,i}$ are listed in Table II. The simulated reflection coefficient of the dipole is shown in Figure 5(b), where the solid and dashed lines represent the magnitude and phase, respectively. The magnitude of the error between the model and the simulation is also plotted in Figure 5(b). The maximum error is -59.4 dB and the average error is -68.8 dB.

The model in (17) satisfies (2) at $s_0 = 0$. We apply the Bode-Fano bound to the model to obtain:

$$\int_{\omega_1}^{\omega_2} \omega^{-2} \log \frac{1}{|\Gamma(j\omega)|} d\omega \le 3.37 \times 10^{-10}, \tag{18}$$

where $\omega_1 = 2\pi \times 10^9$ rad/s and $\omega_2 = \pi \times 10^{10}$ rad/s.

We then follow the steps to compute the improved bound (18). The curves of $|S_L(s)| = 1$ are plotted in Figure 6, together with the poles and zeros of $S_L(s)$. Observing Figure 6, we find $z_{L,1}, z_{L,2} = (-3.01 \pm 9.36j) \times 10^9$ are inside simple closed contours of $|S_L(s)| = 1$ in the LHP. For example, the zoomed-in plot in Figure 6 shows the location of $z_{L,1}$; Ω_1 is defined as the green region containing $z_{L,1}$. Note $z_{L,2}$ and Ω_2 are the complex conjugate of $z_{L,1}$ and Ω_1, and are not shown. Then $\hat{z}_{1,2}$ can be found by optimizing (14) numerically, where $g(z_i) = -\pi/z_i$ (see Table I). The result is $\hat{z}_{1,2} = (-2.95 \pm 9.50j) \times 10^9$. Finally, the improved bound is obtained as

$$\int_{0}^{\infty} \omega^{-2} \log \frac{1}{|\Gamma(j\omega)|} d\omega \le 1.50 \times 10^{-10}. \tag{19}$$

Clearly (19) is more than 50% tighter than (18).

Generally, the amount of improvement in the bound depends on the degree of the rational function approximation—higher degrees tend to allow more improvement.

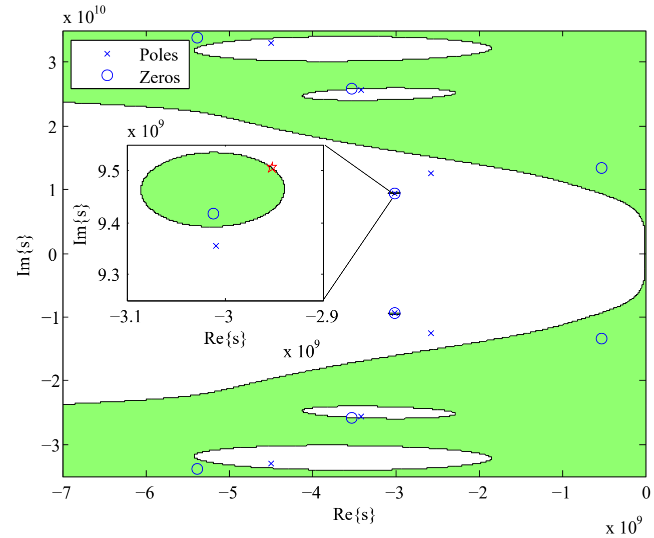

Fig. 6. For the dipole in Figure 5(a) described by (17), $|S_L(s)| = 1$ curves are drawn over the s-plane, and $|S_L(s)| < 1$ regions are filled with green. The zoomed-in plot shows Ω_1, $z_{L,1}$ and $\hat{z}_1$; Ω_2, $z_{L,2}$ and $\hat{z}_2$ are at the complex conjugate locations (not shown).

V. Conclusions

We have presented a method to identify when the Bode-Fano bound cannot be achieved, and presented a technique for tightening the bound. The improved bound can be applied in all cases where the original bound applies, and requires no additional assumptions on the load structure or behavior. Only a few additional mathematical steps are needed. We presented analytical and numerical examples to illustrate its application, and showed that the improvement can be dramatic.

The Bode-Fano bound is applied in practical matching problems in many ways: to guide the design of broadband antennas; to judge whether a prescribed matching bandwidth is realizable; to determine if a matching network is near-optimal. Since our method tightens the bound without imposing any additional conditions or assumptions, it applies just as readily to these same problems.

Whether the improved bound is tight depends on the characteristics of the load and the degree of its rational approximation. We do not know a systematic way to tell this in all cases, and we think this would be an interesting research problem to examine. We also believe a multiport version of this improved bound would be of great interest. Recent results in multiport bounds [8], [9] might be amenable to the analysis presented herein.

References

[1] H. W. Bode, *Network Analysis and Feedback Amplifier Design,* New York, NY, USA: Van Nostrand, 1945.

[2] R. M. Fano, "Theoretical limitations on the broadband matching of arbitrary impedances," *Journal of the Franklin Institute,* 249(1) pp. 57–83, and 249(2), pp. 139–154, 1950.

[3] D. C. Fielder, "Broad-band matching between load and source systems," *IRE Trans. Circ. Thy.,* vol. CT-8, no. 2, pp. 138–153, Jun. 1961.

[4] D. C. Youla, "A new theory of broad-band matching," *IEEE Trans. Circ. Thy.,* vol. CT-11, no. 1, pp. 30–50, Mar. 1964.

[5] H. J. Carlin and P. P. Civalleri, "On flat gain with frequency-dependent terminations," *IEEE Trans. Circ. Sys.*, vol. CAS-32, no. 8, pp. 827–839, Aug. 1985.

[6] Z.-M. Wang and W.-K. Chen, "Broad-band matching of multiport networks," *IEEE Trans. Circ. Syst.,* vol. CAS–31, no. 9, pp. 788–796, Sep. 1984.

[7] P. S. Taluja and B. L. Hughes, "Diversity limits of compact broadband multi-antenna systems," *IEEE J. Sel. Areas Commun.,* vol. 31, no. 2, pp. 326–337, Feb. 2013.

[8] D. Nie, B. M. Hochwald, "Broadband matching bounds for coupled loads," *IEEE Trans. Circ. Sys. I: Reg. Pap.,* vol. 62, no. 4, pp. 995–1004, April 2015.

[9] D. Nie and B. M. Hochwald, "Bandwidth analysis of multiport radio-frequency systems, Parts I & II," *IEEE Trans. Ant. Prop.*, vol. 65, no. 3, pp. 1081–1107, Mar. 2017.

[10] D. Nie and B. M. Hochwald, "Improved Bode-Fano broadband matching bound," *2016 IEEE Ant. Prop. Soc. Int'l Symp. (APS/URSI)*, pp. 179–180, Jun. 26–Jul. 1, 2016.

[11] E. Green, "Synthesis of ladder networks to give Butterworth or Chebyshev response in the pass band," *Proc. IEE III, Radio Commun. Eng.,* vol. 101, no. 70, pp. 115–118, Mar. 1954.

[12] G. Matthaei, "Synthesis of Tchebycheff impedance-matching networks, filters, and interstages," *IRE Trans. Circ. Thy.,* vol. 3, no. 3, pp. 163–172, Sept. 1956.

[13] L. Weinberg and P. Slepian, "Takahasi's results on Tchebycheff and Butterworth ladder networks," *IRE Trans. Circ. Thy.,* vol. CT-7, no. 2, pp. 88–101, Jun. 1960.

[14] R. Levy, "Explicit formulas for Chebyshev impedance-matching networks, filters and interstages," *Proc. IEEE*, vol. 111, no. 6, pp. 1099–1106, June 1964.

[15] H. J. Carlin, "A new approach to gain-bandwidth problems," *IEEE Trans. Circ. Sys.*, vol. 24, no. 4, pp. 170–175, April 1977.

[16] H. J. Carlin and P. Amstutz, "On optimum broad-band matching," *IEEE Trans. Circ. Sys.*, vol. CAS-28, no. 5, pp. 401–405, May 1981.

[17] H. J. Carlin and B. S. Yarman, "The double matching problem: Analytic and real frequency solutions," *IEEE Trans. Circ. Sys.*, vol. CAS-30, no. 1, pp. 15–28, Jan. 1983.

[18] J. W. Helton, "Broadbanding: gain equalization directly from data," *IEEE Trans. Circ. Sys.*, vol. 28, no. 12, pp. 1125–1137, Dec. 1981.

[19] D. F. Schwartz and J. C. Allen, "Wide-band impedance matching: H^∞ performance bounds", *IEEE Trans. Circ. Sys. II: Exp. Briefs,* vol. 51, no. 7, pp. 364–368, Jul. 2004.

[20] A. Ghorbani, R. A. Abd-Alhameed, N. J. McEwan and D. Zhou, "An approach for calculating the limiting bandwidth-reflection coefficient product for microstrip patch antennas," *IEEE Trans. Ant. Prop.*, vol. 54, no. 4, pp. 1328–1331, Apr. 2006.

[21] J. C. Allen and J. Meloling, "Fano bounds for compact antennas: Phase I," SSC San Diego, San Diego, CA, USA, Tech. Rep. 1962, Oct. 2007.

[22] J. Rahola, "Optimization of matching circuits for antennas," *Proc. 5th Euro. Conf. Ant. Prop. (EUCAP),* pp. 776–778. Apr. 11–15, 2011.

[23] P. Henrici, *Applied and Computational Complex Analysis, Volume 1,* Hoboken, NJ, USA: Wiley, 1993.

[24] P. I. Richards, "Resistor-transmission-line circuits," *Proc. IRE*, vol. 36, no. 2, pp. 217–220, 1948.

[25] L. Besser and R. Gilmore, *Practical RF circuit design for modern wireless systems, vol. 1: Passive circuits and systems* Norwood, MA: Artech House, 2003.

[26] J. Helton and O. Merino, *Classical Control Using H^∞ Methods*, Society for Industrial and Applied Mathematics, 1998.

[27] R. W. Newcomb, *Linear Multiport Synthesis,* New York, NY: McGraw-Hill, 1966.

[28] V. Belevitch, *Classical Network Theory,* San Francisco, CA: Holden-Day, 1968.

[29] M. R. Wohlers, *Lumped and Distributed Passive Networks: A Generalized and Advanced Viewpoint,* New York, NY: Academic Press, 1969.

[30] B. Gustavsen and A. Semlyen, "Rational approximation of frequency domain responses by vector fitting," *IEEE Trans. Power Del.,* vol. 14, no. 3, pp. 1052–1061, July 1999.

[31] B. Gustavsen, "Improving the pole relocating properties of vector fitting," *IEEE Trans. Power Del.,* vol. 21, no. 3, pp. 1587–1592, July 2006.

[32] D. Deschrijver, M. Mrozowski, T. Dhaene and D. De Zutter, "Macromodeling of multiport systems using a fast implementation of the vector fitting method," *IEEE Micro. Wireless Comp. Let.,* vol. 18, no. 6, pp. 383–385, June 2008.

[33] B. Gustavsen and A. Semlyen, "Fast passivity assessment for S-parameter rational models via a half-size test matrix," *IEEE Trans. Micro. Thy. Tech.,* vol. 56, no. 12, pp. 2701–2708, Dec. 2008.

[34] B. Gustavsen, "Fast passivity enforcement for S-parameter models by perturbation of residue matrix eigenvalues," *IEEE Trans. Adv. Pack.,* vol. 33, no. 1, pp. 257–265, Feb. 2010.

[35] S. Skogestad and I. Postlethwaite, *Multivariable Feedback Control: Analysis and Design,* 2nd ed., Hoboken, NJ: Wiley, 2005.

Ding Nie Ding Nie (M'16-) was born in Nanchang, Jiangxi, Peoples Republic of China. He received the B.S. degree in electronic engineering from Shanghai Jiao Tong University, Shanghai, in 2010. He received the M.S. degree and the Ph.D. degree in electrical engineering from the University of Notre Dame, Notre Dame, IN, USA, in 2016. He then joined Apple Inc., Cupertino, CA, USA, in 2016. He won the 2016 Outstanding Young Author Award for the paper he co-authored in the IEEE Transactions on Circuits and Systems. His research interests include communications, radio-frequency circuits and antennas.

Bertrand M. Hochwald Bertrand M. Hochwald (F'08-) was born in New York, NY. He received his undergraduate education from Swarthmore College, Swarthmore, PA. He received the M.S. degree in electrical engineering from Duke University, Durham, NC, and the M.A. degree in statistics and the Ph.D. degree in electrical engineering from Yale University, New Haven, CT.

From 1986 to 1989, he worked for the Department of Defense, Fort Meade, MD. After completing graduate school he was a Research Associate and Visiting Assistant Professor at the Coordinated Science Laboratory, University of Illinois, Urbana-Champaign. In September 1996, he joined the Mathematics of Communications Research Department at Bell Laboratories, Lucent Technologies, Murray Hill, NJ where he was a Distinguished Member of the Technical Staff.

In 2005 he joined Beceem Communications, Santa Clara, CA, as their Chief Scientist, and in 2009 as Vice-President of Systems Engineering. He served concurrently as a Consulting Professor in Electrical Engineering at Stanford University, Palo Alto, CA. In 2011, he joined the faculty at the University of Notre Dame as Freimann Professor of Electrical Engineering.

He received several achievement awards while employed at the Department of Defense and the Prize Teaching Fellowship at Yale University. He has served as an Editor for several IEEE journals and given plenary and invited talks on various aspects of signal processing, communications, and radio-frequency systems. He has co-invented several well-known multiple-antenna techniques, including differential methods, linear dispersion codes, and multi-user vector perturbation methods. He has forty-seven patents.

He received the 2006 Stephen O. Rice Prize for the best paper published in the IEEE Transactions on Communications. He co-authored a paper that won the 2016 Best Paper Award by a young author in the IEEE Transactions on Circuits and Systems. He is listed as a Thomson Reuters Most Influential Scientific Mind in 2014 and 2015. He is a Fellow of the IEEE.